Article

Not peer-reviewed version

Development of Chitosan Membrane Reinforced With Hydroxy-Apatite Derived From *Pterygoplichthys* spp (Armored Catfish)

Jorge Humberto Luna-Domínguez , Ana María Mendoza-Martínez * , Ronaldo Câmara-Cozza , Ana Carolina Anzures-Mendoza

Posted Date: 8 February 2024

doi: 10.20944/preprints202402.0494.v1

Keywords: Hydroxyapatite; armored catfish; chitosan membrane; tissue regeneration

Article

Development of Chitosan Membrane Reinforced with Hydroxyapatite Derived from Pterygoplichthys spp (Armored Catfish)

Jorge Humberto Luna-Domínguez [1], Ana María Mendoza-Martínez [2,*], Ronaldo Câmara-Cozza [3,4] and Ana Carolina Anzures-Mendoza [2]

[1] Universidad Autónoma de Tamaulipas. Av. Universidad esq. con Blvd. Adolfo López Mateos, S/N Tampico, C.P. 89337, Tamaulipas, México
[2] Tecnológico Nacional de México- Instituto Tecnológico de Ciudad Madero, Centro de Investigación en Petroquímica, Bahía de Aldahir, Altamira, Tams. México.
[3] University Center of FEI – Ignatian Educational Foundation "Priest Sabóia de Medeiros" Department of Mechanical Engineering. Av. Humberto de Alencar Castelo Branco, 3972 – 09850-901, São Bernardo do Campo, SP – Brazil
[4] CEETEPS - State Center of Technological Education "Paula Souza", Department of Mechanical Manufacturing. Av. Antônia Rosa Fioravante, 804, 09390-120, Mauá, SP, Brazil
* Correspondence: ana.mm@cdmadero.tecnm.mx

Abstract: Nowadays, there is an icreasing interest in the development of novel bioresorbable membranes for Guided Bone Regeneration (GBR). Hydroxyapatite of different resources in combination with chitosan has been used successfully. In this work, armored catfish (Pterygoplichthys spp) bone as a source of hydroxyapatite is proposed; it was isolated through bone calcination at a temperature of 1000 °C. The hydroxyapatite obtained was analyzed for its chemical composition by means of Energy Dispersive Spectroscopy (EDS), its functional groups by Fourier Transform Infrared Spectroscopy (FT-IR), its crystallographic structures were analyzed by X-ray diffraction (DRX) and Scanning electron microscopy (SEM) was used to observe the morphology of the particle. The composed membrane presents a major roughness morphology surface than the pristine chitosan membrane. The hydroxyapatite particles added to the polymeric matrix increased the mechanical tensile properties of the membrane. These findings confirm that armored catfish bones are a viable, economic, and environmentally friendly source of hydroxyapatite, which combined with chitosan, is a suitable alternative to develop biocompatible GBR membranes after it is combined with chitosan.

Keywords: hydroxyapatite; armored catfish; chitosan membrane; tissue regeneration

1. Introduction

Armored catfish (Pterygoplichthys spp) are found in countries located in the Gulf of México [1] as well as in the Asian continent [2]. They are used to clean the bottom of aquariums and control algae growth. Nowadays, this specie is widely spread in the sea and the rivers [3]. Its presence originates some damage to marine fauna, anglers; food search, furthermore, they unravel some plants like those that Vallisneria americana found in wetlands [4]. Its reproduction is very easy, thus putting at risk the ecological balance; its size ranges from 11 to 367 mm, and they can survive in brackish environments increasing the risk of their dispersion [3]. Moreover, its human consumption is not well established; but it is well known that fishbone is mainly composed of hydroxyapatite (HA), a biomaterial with plenty of applications.

Hydroxyapatite is the main mineral component of hard tissues [5]. It is widely used as a bone graft substitute in orthopedic, dental, and maxillofacial applications due to its bioactivity, osteoconductivity, and osteoinductivity [7,8]. The bones used to extract the HA are generally

 doi:10.20944/preprints202402.0494.v1

obtained from residues; this generates a positive impact on the economy and environment by adding high value to an organic resource [6,9–13]. The present work, propose armored catfish bone to develop materials with bioactivity and biocompatibility; particularly, for repairing bone defects in the promising Guided Bone Regeneration (GBR) technique. Furthermore, its use might help to diminish the invasive species.

In guided bone regeneration technique (GBR), membranes are mainly used to cover the defect area; these prevent the connective-tissue cells migration as fibroblast, allowing the growth of bone cells [14–17]. Therefore, the membrane is a fundamental component of the GBR technique. Currently, according to their stability in the body, resorbable and non-resorbable membranes are utilized in GBR therapy; those developed with resorbable natural polymers are more attractive for use in a wider spectrum of clinical situations [18], these avoid a second surgical intervention [4,19–21]. Among the variety of bioresorbable polymers, chitosan (CS) has been reported to have a good affinity with the periodontal ligament cells; it also has a similar structure to glycosaminoglycans that resemble those of the bone tissue extracellular matrix, which facilitates the osteoblast attachment [22–24]. However, pristine chitosan membranes lack osteoinduction and the mechanical properties may be not suitable [25–27]. To further improve the osteoinductive properties and the capacity to prevent the migration of epithelial cells to the socket, the incorporation of calcium phosphates into the CS matrix has been applied as a promising strategy [28–31]. HA obtained from the bone of armored catfish may play this role.

The HA powder was isolated from the bone calcination (1000 °C) of armored catfish (Pterygoplichthys spp). The HA was studied structurally and morphologically, and its elemental composition was found. Then, HA particles into a chitosan matrix (membrane) were incorporated; and the mechanical properties, roughness, and cytotoxicity of the membranes were evaluated as potential materials for GBR.

2. Materials and Methods

Preparation of Hydroxyapatite from armored catfish

Hydroxyapatite was isolated from the armored catfish (Pterygoplichthys spp.) bone. The specimens were collected at the Champayán lagoon situated in Tampico Tamaulipas, México. The fish bones were washed with un-distilled natural water for degreasing and dried at 80 °C for 6 h in a conventional oven; afterwards, the bones were cut into pieces to remove the bone marrow and repeat the washing and drying processes. The cortical bone pieces were pulverized using an agate mortar, followed by calcination at 1000 °C for 1.5 h, using a heating rate of 6 °C/min using a furnace (Magma, Renfert) in air atmosphere. The white powder obtained was ground and then sieved between 325 and 400 mesh, until a particle size between a 37 μm to 44 μm range was obtained for further characterization.

Preparation of chitosan and chitosan/hydroxyapatite membranes

Chitosan from shrimp shells (deacetyl of ≥ 75%) of 190000–375000 Da (Aldrich Chemistry) was used for the membrane fabrication process. Chitosan in a quantity of 0.2 g was dissolved into 10 mL of 1 M acetic acid solution. Then, 0.4 mL of edible glycerin was added with continuous stirring until obtaining a gel-like mixture. Afterwards, 0.1 g of hydroxyapatite was incorporated into the mixture and stirred for 1 minute. The obtained solution was poured into a Petri dish (100 mm in diameter and 1 mm in thickness) and dried in a conventional oven at 40 °C for 24 h to obtain the chitosan/hydroxyapatite (CS/HA) membrane (Figure 1). The amount of hydroxyapatite in relation to the dry weight of the chitosan was 0.5. The same procedure was carried out without the incorporation of HA particles for developing a control chitosan membrane [10].

 doi:10.20944/preprints202402.0494.v1

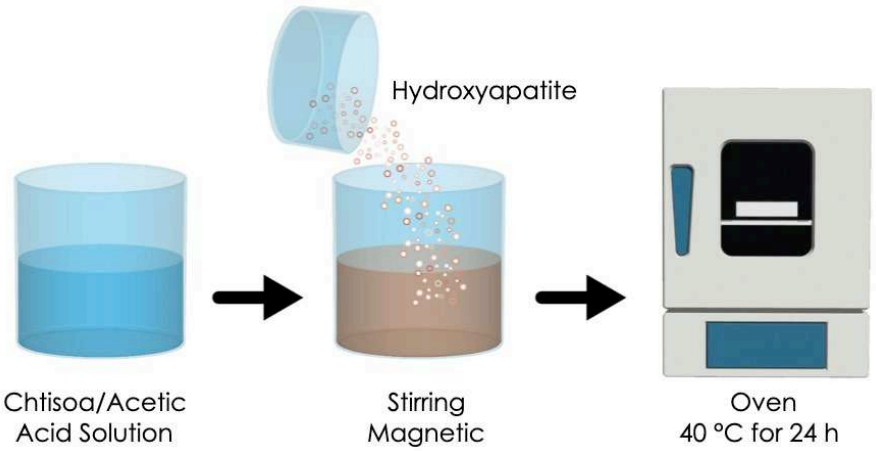

Figure 1. Preparation of chitosan/hydroxyapatite membrane.

Characterization of hydroxyapatite powder and membranes

The phase composition and the crystallinity of HA were evaluated by X-ray diffraction using Bruker D2 phaser equipment with CuK α radiation from 2θ = 20° to 60º in steps of 0.030°. The functional groups of the HA powder and of membranes were identified by an FT-IR Perkin Elmer spectrophotometer using the ATR method and scanned from 4000–650 cm^{-1} with a resolution of 4 cm^{-1}. Scanning electron microscopy (SEM, Jeol JSM 7800F) along with energy dispersive spectroscopy (EDS) was carried out for the HA powder and the membranes surface. The surface roughness of each membrane was determined by a tapping mode using Nanosurf, Naio AFM (Liestal, Switzerland).

Mechanical evaluation of membranes

The evaluation of tensile mechanical properties including the ultimate tensile strength (UTS) and elongation at break (Ɛb) of both membranes was done according to ASTM D 882-02 protocol. Initially, the membranes were cut into specimens of 50×10×1 mm length, width and thickness correspondingly. Subsequently, 8 specimens of each type of membrane were immersed in distilled water at 37 °C in an incubator for 12 hours. They were subjected to a tensile test with an initial velocity of 50 mm/min at room temperature in the MTA Alliance RT/30 universal testing machine equipped with a 5kN static load cell. The ultimate tensile strength and elongation at break were calculated in the software.

In vitro membrane degradation

To characterize the degradation in vitro, the initial weight (Wo) of the membranes was recorded using an electronic balance. Subsequently, the membranes (100 mm in diameter and 1 mm in thickness) were placed in containers filled with artificial saliva solution and then placed in an incubator for 8 weeks at a temperature of 37 °C. Then, the membranes were removed from the artificial saliva and passed by air-drying for 12 hours. The dry weight (Wt) of the membranes was recorded. Therefore, the weight loss (%) record is kept calculated equation 1:

$$Weight\ loss\ (\%) = \left(\frac{Wo - Wt}{Wo}\ x\ 100\right) - 100 \ldots\ldots\ldots\ldots (1)$$

Swelling Analysis

The gravimetric method was used to determine the swelling behavior of the membranes in a controlled implantation environment in vitro [6]. It began by weighing eight dry membranes with the dimension of 20 x 20 mm^2. Subsequently, the membranes were suspended in PBS and incubated at 37 °C for 24 hours. The membranes were removed from the incubator and the excess of PBS from the surface was removed by placing each side of the membranes on filter paper for 60 s. The weight of the wet membranes was recorded again, and the swelling ratio was calculated using equation 2.

$$SR = \frac{(W_w + W_d)}{W_d} * 100 \ldots\ldots\ldots\ldots\ldots (2)$$

Cell Culture

Human gingival fibroblasts (HGF) and osteoblastic cells were prepared from gingival tissues and mandibular bone fragments, obtained by a third molar surgical removal in a 25-year-old patient;

 doi:10.20944/preprints202402.0494.v1

the patient agreed to participate and signed an informed consent document. The tissue samples were prepared in small fragments as follows; they were seeded into 10 cm culture plates and cultured in alpha modification of Eagle's medium (α-MEM, Life Technologies, Gibco, Carlsbad, CA, USA) supplemented with 20% heat-inactivated fetal bovine serum (FBS, Life Technologies, Gibco). To this solution were added 100 UI/mL of penicillin, and 100 mg/mL of streptomycin (Life Technologies, Gibco). The main culture was incubated at 37 °C in a humidified atmosphere with 5% CO_2 until reaching a cell population of 80% of the plate. Then, the cells were harvested by treatment with 0.25% trypsin/ 0.025% ethylenediaminetetraacetic acid disodium salt in phosphate-buffered saline [PBS]. Afterwards the cells were used subculture in α-MEM (LifeTechnologies, Gibco) supplemented with 10% FBS and antibiotics in a humidified atmosphere with 5% CO_2.

Cytotoxicity assay

Cells (2 x 105 cells/ml) were inoculated into 96-microwell plates and incubated for 48 h to achieve complete cell adhesion. The membranes were placed at the bottom of the culture plate and incubated for 24, 48, 72, and 96 h. Cell Proliferation Kit I (MTT) (Sigma-Aldrich, St Louis, MO, USA) was used to determine the number of viable cells. Once the culture medium was replaced by MTT (0.2 mg/mL) dissolved in DMEM, the cells were incubated for 4 h at 37 °C. The formazan product was dissolved with dimethyl sulfoxide (DMSO, Sigma-Aldrich), and the absorbance of the lysate was determined at 540 nm using a microplate reader (Thermo Scientific, St. Louis, MO, USA). Finally, the mean value of the 50% cytotoxic concentration (CC50) of CS/HA membrane and CS membrane was calculated by triplicate from three independent experiments.

Statistical analysis

Quantitative Data were recorded descriptively by the mean ± standard deviation. After testing the normal distribution assumption with the Kolmogorov–Smirnov Test, Student's t-test was used to analyze significant differences between the groups. The statistical significance was set at $p<0.05$. IBM SPSS Statistics 23 software (SPSS, Chicago, IL, USA) was used to perform the statistical analysis.

3. Results

Characterization of the Hydroxyapatite isolated from armoured catfish.

Figure 2a shows the X-ray diffraction pattern of the hydroxyapatite powder from the armoured catfish bones heat-treated at 1000 °C for 1 h. The hydroxyapatite characteristic peak corresponds to the (002), (120), (121), (112), (300), (202), (130), (222), (132), (123), (231) and (004) crystal planes (JCPDS card # 96-901-2217) with a hexagonal phase. The FTIR spectrum (Figure 2b) revealed absorption bands at 1088, 1026, and 962 cm^{-1} associated with the triple group of PO_4^{3-}, confirming a typical apatite structure, as reported in the literature [33,34].

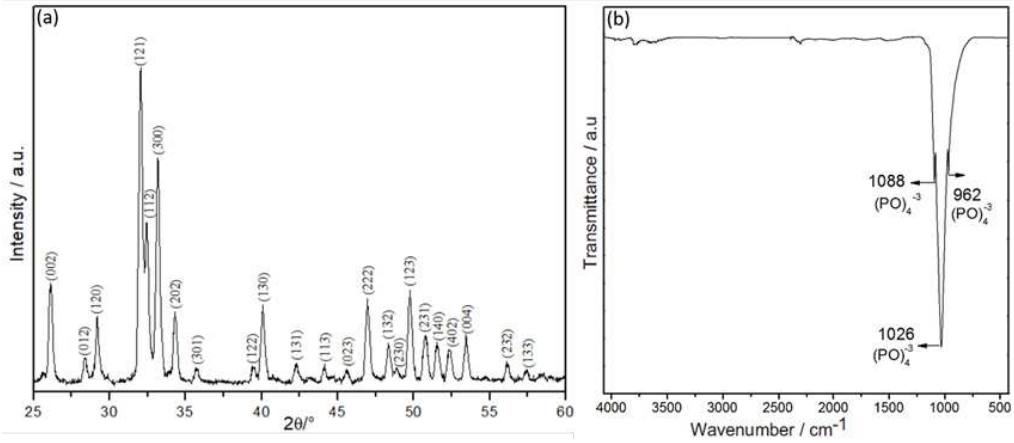

Figure 2. XRD patterns (a) and infrared spectra (b) of hydroxyapatite powder isolated from armoured catfish.

The morphology of the HA powder is shown in Figure 3; rod shapes with a consistent diameter of 0.1–2.0 μm and a length of around 6.0 μm were observed.

 doi:10.20944/preprints202402.0494.v1

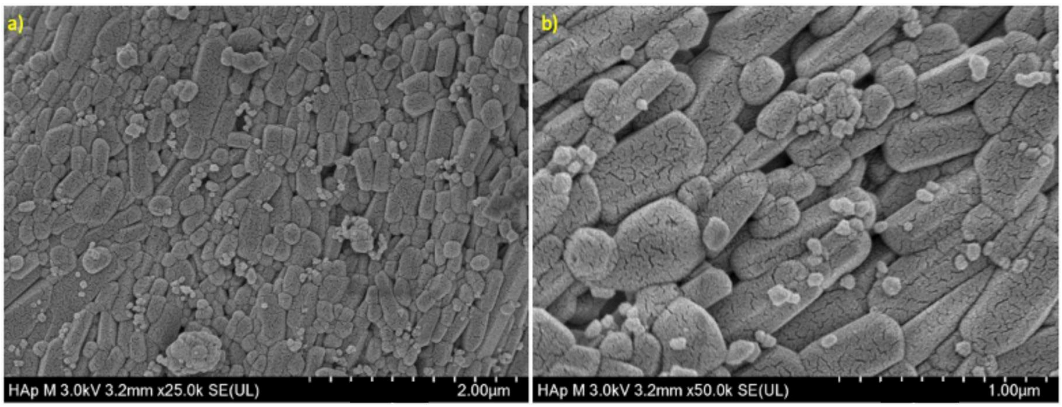

Figure 3. Morphological analyses of hydroxyapatite powder isolated from armored catfish by using SEM (a) 2500x and (b) 5000x.

Through EDS analysis, it was possible to observe traces of ions such as Na, Mg, and Si in the derived natural hydroxyapatite powder (Figure 4). These minor amounts of elements in the HA network increase the proliferation and differentiation of osteoblasts and mimic even more the inorganic component of human bones [35–37].

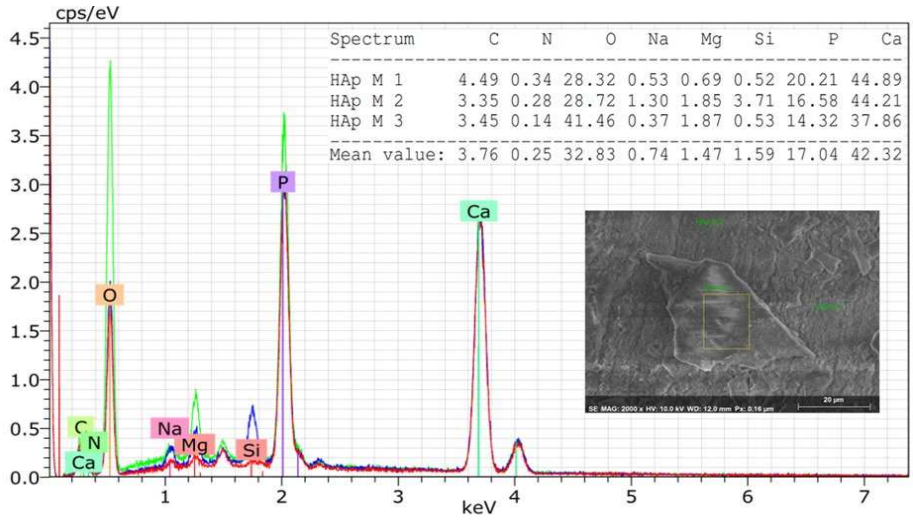

Figure 4. EDS analysis of hydroxyapatite powder isolated from armored catfish.

Characterization of the membranes

The SEM micrograph of the CS/HA (Figure 5a) and the CS membranes (Figure 5b) revealed a dense structure; perhaps, the incorporation of HA particles into the chitosan matrix generates a roughness morphology surface. Whilst a smooth surface was observed on the CS membrane. Likewise, the AFM-3D images are observed in (Figure 5c-d), which also support the differences between the membranes related to the surface topography. The roughness average (Ra) between the membranes found by the AFM analysis is shown in Figure 6. It is important to mention that roughness and porosity allow osteoblast attachment.

 doi:10.20944/preprints202402.0494.v1

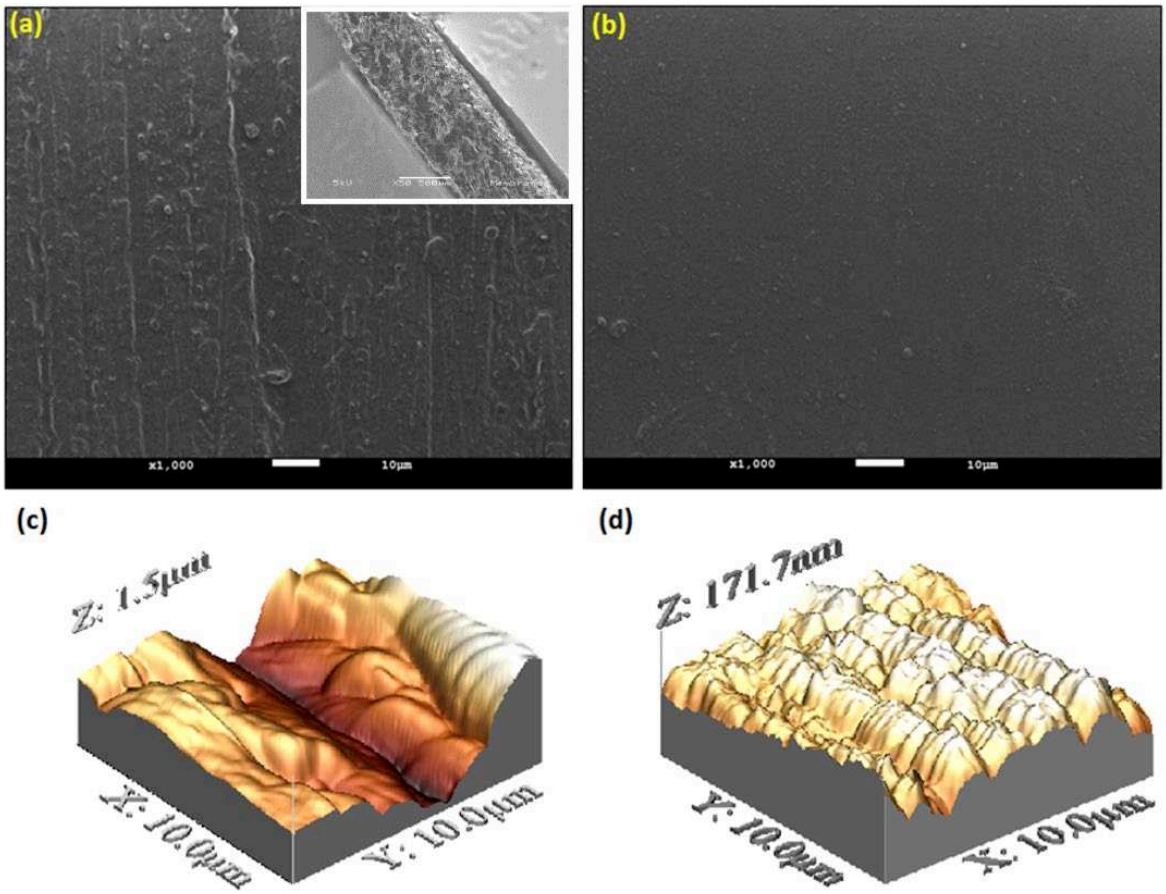

Figure 5. SEM micrographs of CS/HA membrane (a) and CS membrane (b) 1000x. 3D-AFM images of the surface topographical appearance: CS/HA membrane (c) and CS membrane. (Inside figure) cross-section CS/HA membrane.

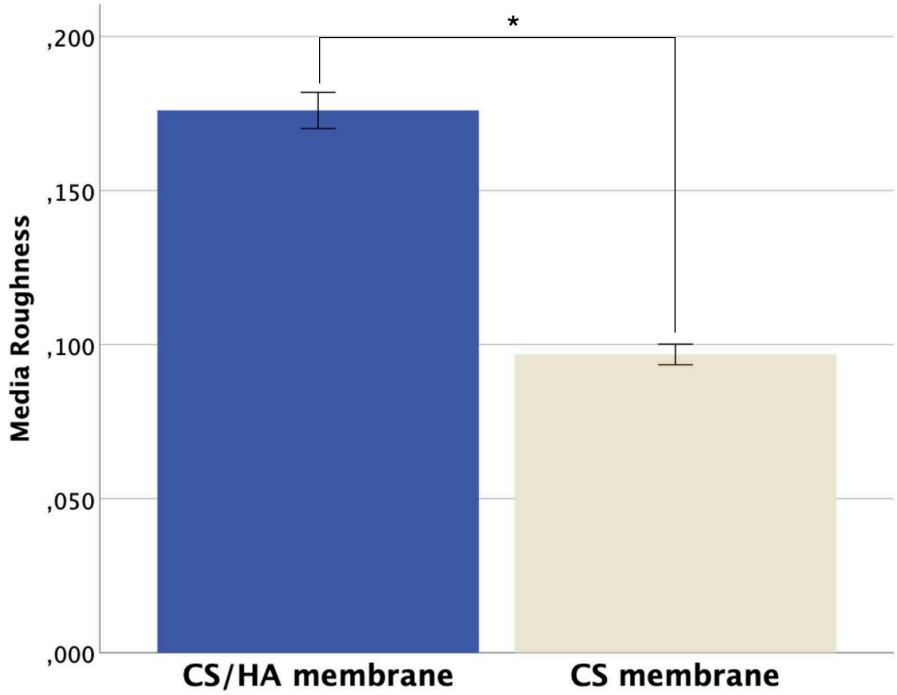

Figure 6. Quantitative roughness surface (Ra) of the CS/HA membrane and CS membrane. The (*) denotes statistically significant difference ($p < 0.001$). Error Bars +/- SD.

 doi:10.20944/preprints202402.0494.v1

The mapping analysis of the elementary composition showed that the CS/HA membrane additionally presents Ca, P, and trace elements such as Mg and Si (Figure 7a) while the CS membrane only presented C, O, and Na (Figure 7b).

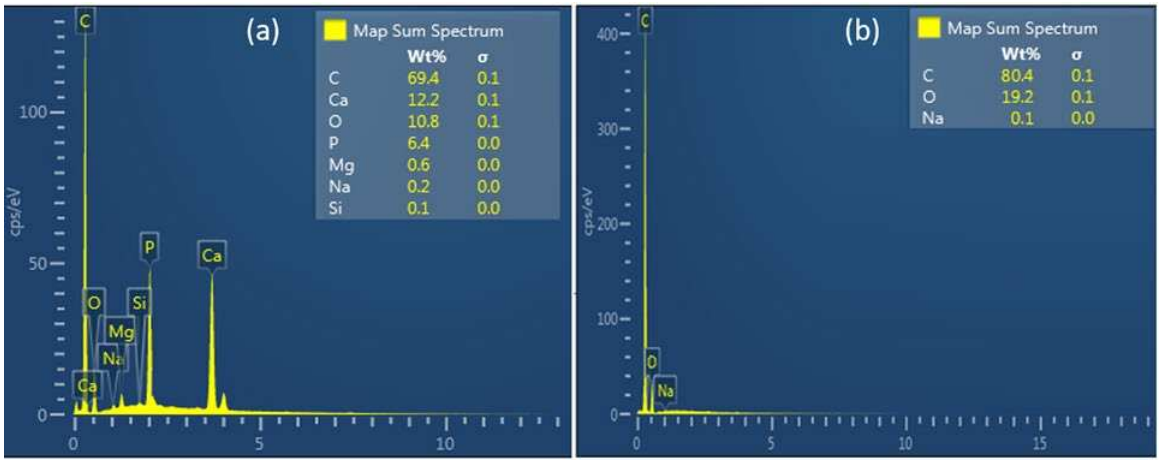

Figure 7. Elemental composition analysis by EDS: CS/HA membrane(a) and CS membrane (b).

Mechanical evaluation of the membranes

Mechanical tensile properties found in the CS/HA membrane are summarized by descriptive statistics in Table 1.

Table 1. Tensile mechanical properties include ultimate tensile strength (UTS) and elongation at break (εb) of CS/HA membrane and CS membrane. Data represent mean ± Standard Deviation. * Statistically significant difference.

	CS/HA Membrane	CS Membrane	*p value*
UTS (MPa)	5.4 ± 0.62	3.3 ± 0.46	*<0.001**
Ɛb (%)	92.4 ± 5.2	54 ± 6.1	*<0.001**

In vitro degradation and Swelling analysis

Table 2 shows the percentage of weight loss of the membranes after 8 weeks. The CS/HA membranes presented an average percentage weight loss of 43.7% while the CS membranes presented a loss of 54.2%.

Table 2. Weight loss (%) after 8 weeks exposed to artificial saliva solution at 37 °C. Swelling behavior for 24 h at 37 °C.

	CS/HA Membrane	CS Membrane	*p value*
Weight loss (%)	54.2 ± 7.1%	43.7 ± 5.92%	*<0.001**
Swelling Ratio (%)	62.5 ± 3.0%	54.4 ± 3.3%	*0.004**

The results obtained from the swelling analysis showed that the CS/HA membrane presents an increase in the water absorption capacity compared to the CS membrane. Table 3.

Table 3. Cytotoxicity of a CS/HA membrane and CS membrane in direct contact with osteoblasts and human gingival fibroblasts at different times.

 doi:10.20944/preprints202402.0494.v1

Viability (%)	Control	CS/HA Membrane	CS Membrane
	Osteoblasts		
24 h	100 ± 9.8	88 ± 11.4	89 ± 12
48 h	100 ± 8.3	84 ± 8.1	85 ± 7.7
72 h	100 ± 4.2	81 ± 6.9	82 ± 6.1
96 h	100 ± 1.3	78 ± 4.7	81 ± 4.2
	Human Gingival Fibroblasts		
24 h	100 ± 4	89 ± 7.8	87 ± 7.1
48 h	100 ± 3.1	87 ± 6.4	83 ± 4.9
72 h	100 ± 1.6	83 ± 4.1	81 ± 3.7
96 h	100 ± 0.8	81 ± 2.2	79 ± 2.8

Cytotoxicity assay

The cell viability results for both membranes in direct contact with osteoblasts and human gingival fibroblasts showed a similar reduction of cell viability of less than 30% in the evaluated periods. No statistically significant difference was detected on the cell viability between both membranes. ($p > 0.05$). Table 3.

4. Discussion

The diffractogram of the hydroxyapatite powder from the armoured catfish bones revealed narrow high-intensity peaks, which could be associated with larger crystallite sizes [38]. This behavior has also been observed in calcined tuna bones at temperatures above 700 °C, which indicates that the organic material has been eliminated [34]. The main intensities correspond to the planes (002), (120), (121), (112), (300), (202), (130), (222), (132), (123), (231) and (004); these results are consistent with those obtained for synthesized nano-HA [38]. The XRD result was correlated with the FTIR study. At the treated temperature (1000 °C), it was completely removed the organic matter without decomposing the hexagonal HA phase, therefore, HA has been obtained. Similar results have been reported for Sheelavati fish and bovine bones [39,40]. Bands in 2034 and 2157 cm-1 were found in the tuna bones at the same temperature [41], however, these bands were not exhibited for armored catfish of this work. Rod-shaped particles with small pores on their surface were obtained for armored catfish HA, compared from HA from other natural sources, which shown rock-shaped but with similar particle size [41]. Similar results were obtained for synthesized nano-HA [38]. It might be possible that rode-shaped morphology may improve the crosslinking in the membrane formation, also, the small pores may ensure tissue growth as well as cell attachment. The average Ca/P ratio was 1.9 ± 0.03. This result agrees with data reported by others, independently of calcination temperature [41]. However, previous studies suggested that Ca/P ratios lower than 1.67 occur in calcination temperatures above 800 °C [37,42], which is not the case for armored catfish H. Ca/P ratios in the range of 0.9 – 1.11 were found in the jaw tissue of Wistar rats; thus, that HA obtained in this study may be used for tissue engineering [43]. It has been reported that calcination treatments between 900 °C and 1100 °C led to partial decomposition of the hydroxyapatite phase in tricalcium phosphate, a phenomenon that in this study was not observed according to the DRX pattern [6,44]; this is also confirmed by FTIR spectrum, where additional absorption bands do not appear. The likely explanation for this phenomenon is that the main inorganic component of the armored catfish bones is a non-stoichiometric HA without calcium deficiency.

Uniformly distributed cylindrical formations are observed in the CS/HA membrane, which can be attributed to the rod shape of the HA particles, which in turn are aligned. A smooth surface was observed on the CS membrane. The AFM-3D images support the differences between the membranes related to the surface topography. Very similar results have been reported for chitosan matrix prepared with different calcium phosphate particles [29,45]. Moreover, a statistically significant difference in the roughness average (Ra) between the membranes was found. The CS/HA membrane present higher roughness values (Ra) than the CS membrane, 0.176 ± 0.006 and 0.097 ±

 doi:10.20944/preprints202402.0494.v1

0.003, respectively ($p < 0.001$) (Figure 5). Roughness and porosity allow osteoblastic attachment; according to the literature, biomaterials with a surface roughness (Ra) greater than 0.2 promote the accumulation of bacteria that cause inflammation and delay the defect bone healing [45–47]. Fortunately, the simple method proposed for the development of the CS/HA membrane allows for the maintenance of adequate roughness. The mapping analysis of the elementary composition showed that the CS/HA membrane presents Ca, P, and trace elements such as Mg and Si; while the CS membrane only presented C, O, and Na. Therefore, according to these results, it is assumed that this composite membrane increases its mechanical integration with bone tissue and cell adhesion by facilitating the chelation of the cation's chemical interactions [48].

Regarding the final tensile strength, the CS/HA membrane score was 1.64 times higher than the CS membrane ($p < 0.001$). In addition, the reported elongation at break in the CS/HA membrane increased to approximately 92.4% while the CS membrane was about 54% ($p < 0.001$). This improvement is associated with the addition of hydroxyapatite particles into the chitosan. Instead of just dispersing, the particles might be mainly cross-linked to the polymeric matrix chains; this effect may be associated with the rod shape of the HA particles. According to the literature, positively charged chitosan amine groups as well as their deprotonated portion can lead to attraction by electrostatic forces with negatively charged PO_4^{3-} ions and cationic Ca ions present in the hydroxyapatite [6,9,48]. The ultimate tensile strength of the CS/HA membrane (5.4 Mpa) is a little superior to that of commercial collagen membranes of natural origin (4.8 Mpa) [49]; biodegradable PLGA membranes reported in the literature also have lower performance (4.57 Mpa) [50]. The elongation at break increased from 54% to 92.4% for CS membrane and CS/HA membrane, respectively; these values are within the range of other chitosan-based membranes [29]. The results of the present study showed that the dispersion of HA (1% w/v) in a chitosan solution (2% w/v) allowed to increase the degradation rate and the fluid absorption capacity. This may be since the amount of HA microparticles that were incorporated into the chitosan matrix inhibited the entanglement of its chains and weakened its intermolecular hydrogen bonds. Therefore, this generates spaces for the penetration of water and a greater exposure of free hydrophilic groups for the interaction of water molecules [6]. Furthermore, this increase in the fluid absorption capacity is possibly related to the hydrolysis of chitosan and therefore increases the rate of degradation.

The cell viability results of each membrane indicate a non-cytotoxic effect (less than 30% in the evaluated periods); this asseveration is based on the interpretation of the ISO 10993-5: Biological evaluation of medical devices. In vitro cytotoxicity tests (Table 2). HA resulted in better membrane performance for the human gingival fibroblasts.

Consequently, armored catfish bone added to a chitosan matrix may be an alternative for the development of biodegradable membranes for GBR. This proposal could help to diminish the impact of this invasive and dangerous specie. Likewise, to reach a commercial product, there are necessary additional studies, like biodegradability, which will be addressed in future work, biocompatibility testing and other in vivo studies.

5. Conclusions

In this study, the armored catfish (Pterygoplichthys spp) bone has been successfully used for the first time as a source of isolated calcium phosphate hydroxyapatite phase. The bone was treated at 1000 °C. From the XRD analysis, it was observed a diffractogram corresponding to the hexagonal structure. The FTIR spectra revealed the typical PO_4^{3-} absorption confirming apatite structure. In addition, the average Ca/P ratio was found as 1.9 ± 0.03 and the presence of trace elements such as Si and Mg can improve the biological performance of the HA powder. Moreover, it was concluded that the incorporation of HA particles into a CS membrane enhances the barrier function properties and the bone promoting capacity. The chemical interactions between HA and the chitosan matrix chains increased the mechanical tensile properties of the membrane. The CS/HA membrane has no cytotoxic effect in direct contact with osteoblasts and human gingival fibroblasts. Despite the promising results obtained with the CS/HA membrane, should be explored the alternative to

incorporate materials such as whitlockite and ZnO to allow the attraction of osteogenic proteins and improve the antibacterial properties, and in vivo studies as well.

Author Contributions: "Formal analysis, Jorge Luna-Domínguez, Ana Mendoza-Martínez and Ronaldo Câmara-Cozza; Investigation, Ana Mendoza-Martínez and Ana Anzures-Mendoza; Resources, Jorge Luna-Domínguez; Software, Jorge Luna-Domínguez and Ronaldo Câmara-Cozza; Validation, Jorge Luna-Domínguez and Ana Mendoza-Martínez; Visualization, Ronaldo Câmara-Cozza and Ana Anzures-Mendoza; Writing – original draft, Jorge Luna-Domínguez and Ana Mendoza-Martínez; Writing – review & editing, Ana Mendoza-Martínez. All authors have read and agreed to the published version of the manuscript.".

Funding: This research received no external funding.

Acknowledgments: The authors acknowledge SNI-CONACYT and SIP-IPN (20220462) for supporting this work. The authors are also indebted to CIFO-UAT. HHC acknowledges the financial support from VIEP-BUAP, México. A.M.M.M. is grateful to Tecnológico Nacional de México-Instituto Tecnológico de Ciudad Madero for her sabbatical authorization.

Conflicts of Interest: The authors declare no conflict of interest.

References

1. Wakida-Kusunoki, A.T; Ruiz-Carus, R.; Amador del Angel, L.E. Amazon sailfin catfish, Pterygoplichthys pardalis (Castelnau, 1855) (Loricariidae), another exotic species established in Southeastern Mexico. Southwestern Natur. 2007, 52, 141–144. DOI:10.1894/0038-4909(2007)52[141:ASCPPC]2.0.CO;2
2. Wu, L. W.; Liu, C. C.; Lin, S. M. Identification of exotic sailfin catfish species (Pterygoplichthys, Loricariidae) in Taiwan based on morphology and mtDNA sequences. Zoolog. St. 2011, 50, 235–246.
3. Capps, K.A.; Nico, L.G.; Mendoza-Carranza, M.; Arévalo-Frías, W.; Ropicki, A.; Heilpern, S.A.; Rodiles-Hernández, R. Salinity tolerance of non-native suckermouth armoured catfish (Loricariidae: Pterygoplichthys) in Southeastern Mexico: Implications for invasion and dispersal. Aqu. Cons.: Mar. Freshw. Ecosyst. 2011, 21, 528–540. DOI: 10.1002/aqc.1210
4. Hoover, J.J.; Killgore, K.J.; Cofrancesco, A.F. Suckermouth catfishes: Threats to aquatic ecosystems of the United States? Aqu. Nuis. Spec Res. Bull. 2004, 4, 1–9.
5. Cheng, H.; Chabok, R.; Guan, X.; Chawla, A.; Li, Y. Synergistic interplay between the two major bone minerals, hydroxyapatite and whitlockite nanoparticles, for osteogenic differentiation of mesenchymal stem cells. Acta Biomater. 2018, 69, 342–351. DOI: 10.1016/j.actbio.2018.01.016
6. Bee, S.; Hamid, Z.A.A. Characterization of chicken bone waste-derived hydroxyapatite and its functionality on chitosan membrane for guided bone regeneration. Compos. Part B. 2019, 163, 562–73. DOI:10.1016/J.COMPOSITESB.2019.01.036
7. De Tullio, I.; Caputi, S.; Perfetti, G.; Mavriqi, L.; Wismeijer, D.; Traini, T. A Human Clinical and Histomorphometrical Study on Different Resorbable and Non-Resorbable Bone Substitutes Used in Post-Extractive Sites. Preliminary Results. Materials (Basel). 2019, 12, 2408. doi: 10.3390/ma12152408
8. Monika, Š. Substituted hydroxyapatites for biomedical applications: A review. Ceram. Int. 2015, 41, 9203–9231. DOI:10.1016/j.ceramint.2015.03.316
9. Luna-Domínguez, J.H.; Téllez-Jiménez, H.; Hernández-Cocoletzi, H.; García-Hernández, M.; Melo-Banda, J.A., Nygren, H. Development and in vivo response of hydroxyapatite/whitlockite from chicken bones as bone substitute using a chitosan membrane for guided bone regeneration. Ceram. Int. 2018, 44, 22583–22591. https://doi.org/10.1016/j.ceramint.2018.09.032
10. Mondal, S.; Mondal, B.; Dey, A.; Mukhopadhyay, S.S. Studies on Processing and Characterization of Hydroxyapatite Bio-materials from Different Bio Wastes. J. Miner. Mater. Charact. Eng. 2012, 11, 55–67. DOI: 10.4236/jmmce.2012.111005
11. Saber-Samandari, S.; Saber-Samandari, S.; Ghonjizade-Samani, F.; Aghazadeh, J.; Sadeghi, A. Bioactivity evaluation of novel nanocomposite scaffolds for bone tissue engineering: The impact of hydroxyapatite. Ceram. Int. 2016, 42, 11055–11062. DOI10.1016/j.ceramint.2016.04.002
12. Pon-On, W.; Suntornsaratoon, P.; Charoenphandhu, N.; Thongbunchoo, J.; Krishnamra, N.; Tang, I.M. Hydroxyapatite from the fish scale for potential use as a bone scaffold or regenerative material. Mater. Sci. Eng. C. 2016, 62, 183–189. DOI: 10.1016/j.msec.2016.01.051
13. Kamalanathan, P.; Ramesh, S.; Bang, L.T.; Niakan, A.; Tan, C.Y.; Purbolaksono, J. Synthesis and sintering of hydroxyapatite derived from eggshells as a calcium precursor. Ceram Int. 2014, 40, 16349–16359. DOI10.1016/j.ceramint.2014.07.074
14. Elgali, I.; Omar, O.; Dahlin, C.; Guided, T.P. Guided bone regeneration: materials and biological mechanisms revisited. Eur J Oral Sci. 2017, 315–37. DOI: 10.1111/eos.12364

15. Irinakis, T. Rationale for socket preservation after extraction of a single-rooted tooth when planning for future implant placement. J Can Dent Assoc (Tor). 2007, 72, 917–22.
16. Fenbo, M.; Xingyu. X.; Bin, T. Strontium chondroitin sulfate/silk fibroin blend membrane containing microporous structure modulates macrophage responses for guided bone regeneration. Carbohydr. Polym. 2019, 213, 266–75. DOI: 10.1016/j.carbpol.2019.02.068
17. Rocchietta, I.; Simion, M.; Hoffmann, M.; Trisciuoglio, D.; Benigni, M.; Dahlin, C. Vertical Bone Augmentation with an Autogenous Block or Particles in Combination with Guided Bone Regeneration : A Clinical and Histological Preliminary Study in Humans. Clin Implant Dent Relat Res. 2016, 18, 19–29. DOI: 10.1111/cid.12267
18. Wang, J.; Wang, L.; Zhou, Z.; Lai, H.; Xu, P.; Liao, L.; Wei, J. Biodegradable Polymer Membranes Applied in Guided Bone/Tissue Regeneration: A Review. Polym. 2016, 8, 115-135. DOI: 10.3390/polym8040115
19. Atrian, M.; Kharaziha, M.; Emadi, R.; Alihosseini, F. Silk-Laponite® fibrous membranes for bone tissue engineering. Appl Clay Sci. 2019, 174, 90–9. DOI:10.1016/j.clay.2019.03.038
20. Stankovic, D.; Labudovic-Borovic, M.; Radosavljevic, R.; Marinkovic, M.; Isenovic, E.R. Use of acellular collagen matrix for the closure of the open oral wound in bone regeneration. J. Stomatol. Oral Maxillofac. Surg. 2018, 119, 446–9. Doi: 10.1016/j.jormas.2018.04.015
21. Masoudi Rad, M.; Nouri Khorasani, S.; Ghasemi-Mobarakeh, L.; Prabhakaran M.P.; Foroughi, M.R.; Kharaziha, M.; Saadat-kish, N.; Ramakrishna, S. Fabrication and characterization of two-layered nanofibrous membrane for guided bone and tissue regeneration application. Mater. Sci. Eng. C. 2017, 80, 75–87. DOI: 10.1016/j.msec.2017.05.125
22. Arancibia, R.; Marutana, C.; Silva, D.; Tobar, N.; Tapia, C.; Salazar, J.C.; Martínez, J.; Smith, P.C. Effects of Chitosan Particles in Periodontal Pathogens and Gingival Fibroblasts. J. Dent. Res. 2013, 92, 740–5. DOI: 10.1177/0022034513494816
23. Venkatesan, J.; Kim, S.K. Chitosan composites for bone tissue engineering - An overview. Mar. Drugs. 2010, 8, 2252–66. DOI: 10.3390/md8082252
24. Acevedo, C.A.; Olguín, Y.; Briceño, M.; Forero, J.C.; Osses, N.; Díaz-Calderón, P.; Jaques, A.; Ortiz, R. Design of a biodegradable UV-irradiated gelatin-chitosan/nanocomposed membrane with osteogenic ability for application in bone regen-eration. Mater. Sci. Eng. C. 2019, 99, 875–86. https://doi.org/10.1016/j.msec.2019.01.135
25. Munhoz, M.A.S.; Hirata, H.H.; Plepis, A.M.G.; Martins, V.C.A., Cunha, M.R. Use of collagen/chitosan sponges mineralized with hydroxyapatite for the repair of cranial defects in rats. Injury. 2018, 49, 2154–60. DOI: 10.1016/j.injury.2018.09.018
26. Pereira, I.C.; Duarte, A.S.; Neto, A.S.; Ferreira, J.M.F. Chitosan and polyethylene glycol-based membranes with antibacterial properties for tissue regeneration. Mater. Sci. Eng. C. 2019, 96, 606–15. DOI: 10.1016/j.msec.2018.11.029
27. Cheng, Y.; Hu, Z.; Zhao, Y.; Zou, Z.; Lu, S.; Zhang, B.; Li, S. Sponges of Carboxymethyl Chitosan Grafted with Collagen Peptides for Wound Healing. Int. J. Mol. Sci. 2019, 20, 3890-3902. https://doi.org/10.3390/ijms20163890
28. Chen, P.; Liu, L.; Pan, J.; Mei, J.; Li, C.; Zheng, Y. Biomimetic composite scaffold of hydroxyapatite/gelatin-chitosan core-shell nanofibers for bone tissue engineering. Mater. Sci. Eng. C. 2019, 97, 325–35. DOI: 10.1016/j.msec.2018.12.027
29. Chen, Y.; Tai, H.; Fu, E.; Don, T. Guided bone regeneration activity of different calcium phosphate/chitosan hybrid membranes. Int J Biol Macromol. 2019, 126, 159–69. DOI: 10.1016/j.ijbiomac.2018.12.199
30. Lee, J.S.; Baek, S.D.; Venkatesan, J.; Bhatnagar, I.; Chang, H.K.; Kim, H.T.; Kim, S.K. In vivo study of chitosan-natural nano-hydroxyapatite scaffolds for bone tissue regeneration. Int J Biol Macromol. 2014, 67, 360–6. DOI: 10.1016/j.ijbiomac.2014.03.053
31. Park, K.; Yun, Y.; Kim, S.E.; Song, H. The Effect of Alendronate Loaded Biphasic Calcium Phosphate Scaffolds on Bone Regeneration in a Rat Tibial Defect Model. Int. J. Mol. Sci. 2015, 16, 26738–26753. doi: 10.3390/ijms161125982
32. Saigo, L.; Kumar, V.; Liu, Y.; Lim, J.; Teoh, S.H.; Goh, B.T. A pilot study: Clinical efficacy of novel polycaprolactone-tricalcium phosphate membrane for guided bone regeneration in rabbit calvarial defect model. J. Oral Maxillofac. Surgery, Med. Pathol. 2018, 30, 212–219. DOI:10.1016/j.ajoms.2017.12.007
33. Poinern, G.J.E.; Brundavanam, R.; Le. X.T.; Djordjevic, S.; Prokic, M.; Fawcett, D. Thermal and ultrasonic influence in the formation of nanometer scale hydroxyapatite bio-ceramic. Int. J. Nanomedicine 2011, 2011, 2083–2095. DOI: 10.2147/IJN.S24790
34. Venkatesan J.; Kim, S.K. Effect of Temperature on Isolation and Characterization of Hydroxyapatite from Tuna (Thunnus obesus) Bone. Mater. 2010, 3, 4761-4772. doi: 10.3390/ma3104761
35. Camargo, H.A.N.; de Lima, S.A.; Gemelli, E. Synthesis and Characterization of Hydroxyapatite/TiO2n Nanocomposites for Bone Tissue Regeneration. Am. J. Biomed. Eng. 2012, 2, 41–7. DOI: 10.5923/j.ajbe.20120202.08

36. Bee, S.L.; Mariatti, M.; Ahmad, N.; Yahaya, B.H.; Hamid Z.A.A. Effect of the calcination temperature on the properties of natural hydroxyapatite derived from chicken bone wastes. Mater. Today Proc. 2019, 16, 1876–85. DOI: https://doi.org/ https://doi.org/10.22517/23447214.24888
37. Sunil, B.R.; Jagannatham, M. Producing hydroxyapatite from fish bones by heat treatment. Mater. Lett. 2016, 185, 411–4. DOI10.1016/j.matlet.2016.09.039
38. Shi, P.; Liu, M.; Fan, F.; Yu, C.; Lu, W.; Du, M. Characterization of natural hydroxyapatite originated from fish bone and its biocompatibility with osteoblasts. Mater. Sci. Eng. C. 2018, 90, 706–12. DOI: 10.1016/j.msec.2018.04.026
39. Zainol, I.; Adenan, N.H.; Rahim, N.A.; Jaafar, C.N.A. Extraction of natural hydroxyapatite from tilapia fish scales using alkaline treatment. Mater Today Proc. 2019, 16, 1942–1948. DOI:10.1016/J.MATPR.2019.06.072
40. Henríquez-Távara, N.; García-Molina, J.A.; Machado, G.; Carvalho-Lobato, P.; Belmonte-Calderón, A.; Serra-Renom, I.; Manzanares-Céspedes, M.C. Análisis semicuantitativo del calcio y fósforo en los tejidos calcificados de la mandíbula. Biomec. 2002, 10, 5-13.
41. Mohd Pu'ad, N.A.S.; Koshy, P.; Abdullah, H.Z.; Idris, M.I.; Lee, T.C. Syntheses of hydroxyapatite from natural sources. Heli-yon. 2019, 5, e01588. https://doi.org/10.1016/j.heliyon.2019.e01588
42. Zhu, Q.; Ablikim, Z.; Chen, T.; Cai, Q.; Xia, J.; Jiang, D.; Wang, S. The preparation and characterization of HA/β-TCP biphasic ceramics from fish bones. Ceram Int. 2017, 43, 12213–20. DOI https://doi.org/10.1088/2053-1591/ab5a8f
43. Tai, H.; Fu, E.; Don, T. Calcium phosphates synthesized by reverse emulsion method for the preparation of chitosan composite membranes. Carbohydr Polym. 2012, 88, 904–11. DOI:10.1016/j.carbpol.2012.01.042
44. Chu, C.; Deng. J.; Xiang, L.; Wu, Y.; Wei, X.; Qu, Y.; Man, Y. Evaluation of epigallocatechin-3-gallate (EGCG) cross-linked collagen membranes and concerns on osteoblasts. Mater. Sci. Eng. C. 2016, 67, 386–94. DOI: 10.1016/j.msec.2016.05.021
45. Banerjee, S.; Bagchi, B.; Bhandary, S.; Kool, A.; Hoque, N.A.; Biswas, P.; Pal, K.; Thakuy, P.; Das, K.; Karmakar, P.; Das, S. Antimicrobial and biocompatible fluorescent hydroxyapatite-chitosan nanocomposite films for biomedical applications. Coll. Surf. B: Bioint. 2018, 171, 300–307. DOI: 10.1016/j.colsurfb.2018.07.028
46. Matinfar, M.; Mesgar, A.S.; Mohammadi, Z. Evaluation of physicochemical, mechanical and biological properties of chitosan/carboxymethyl cellulose reinforced with multiphasic calcium phosphate whisker-like fibers for bone tissue engineering. Mater. Sci. Eng. C. 2019, 100, 341–53. DOI: 10.1016/j.msec.2019.03.015
47. Félix, A.; de Almeida Filho, E.; da Silva Rigo, E.C., Ortega Boschi, A. Synthesis of chitosan/hydroxyapatite membranes coated with hydroxycarbonate apatite for guided tissue regeneration purposes. Appl. Surf. Sci. 2011, 257, 3888–92. doi:10.1016/j.apsusc.2010.11.104
48. Sathiyavimal, S.; Vasantharaj, S.; Lewisoscar, F.; Pugazhendhi, A.; Subashkumar, R. Biosynthesis and characterization of hydroxyapatite and its composite (hydroxyapatite-gelatin-chitosan-fibrin-bone ash) for bone tissue engineering applications. Int. J. Biol. Macromol. 2019, 129, 844–52. DOI: 10.1016/j.ijbiomac.2019.02.058
49. Ortolani, E.; Quadrini, F.; Bellisario, D.; Santo, L; Polimeni, A.; Santarsiero, A. Mechanical qualification of collagen membranes used in dentistry. Ann. Ist. Super. Sanità. 2015, 51, 229-235. DOI: 10.4415/ANN_15_03_11
50. Guo, M.; Chu, Z.; Yao, J.; Feng, W.; Wang, Y.; Wang, L.; Fan, Y. The effects of tensile stress on the degradation of biodegradable PLGA membranes: A quantitative study. Polym. Degrad. Stabyl. 2016, 124, 95-100. DOI:10.1016/j.polymdegradstab.2015.12.019
51. Wu, H; Ji, D.; Chang, W.; Yang, J.; Lee, S. Chitosan-based polyelectrolyte complex scaffolds with antibacterial properties for treating dental bone defects. Mater. Sci. Eng. C. 2012, 32, 207–214. DOI 10.1016/j.msec.2011.10.020
52. Kitayama, S.; Wong, L.O.; Ma, L.; Hao, J.; Kasugai, S.; Lang, N.P.; Mattheos, N. Regeneration of rabbit calvarial defects using biphasic calcium phosphate and a strontium hydroxyapatite-containing collagen membrane. Clin. Oral Implants Res. 2016, 27, e206–e214. DOI: 10.1111/clr.12605
53. Vijayakumar, P.; Vathaluru, S.; Abisegapriyan, S.; Sherine, J.; Ramakrishna, S.; Hasbi, M.; Rahim, A.; Mohd, M.; Jose, R.; Reddy, J. Ramification of zinc oxide doped hydroxyapatite biocomposites for the mineralization of osteoblasts. Mater. Sci. Eng. C. 2019, 96, 337–46. https://doi.org/10.1016/j.msec.2018.11.033
54. Nygren, H.; Bigdeli, N.; Ilver, I.; Malmberg, P. Mg-corrosion, hydroxyapatite, and bone healing. Biointerphases. 2017, 12, 02C407-1-02C407-8. DOI: 10.1116/1.4982601
55. Liao, S.; Watari, F.; Zhu,Y.; Uo, M.; Akasaka, T.; Wang, W.; Cui, F. The degradation of the three-layered nano-carbonated hydroxyapatite/collagen/PLGA composite membrane in vitro. Dental Materials. 2007, 23, 1120-1128. DOI: 10.1016/j.dental.2006.06.045.

 doi:10.20944/preprints202402.0494.v1